

Bond-Valence Constraints on Liquid Water Structure

Barry R. Bickmore,^{*,†} Kevin M. Rosso,[‡] I. David Brown,[§] and Sebastien Kerisit[‡]

Department of Geological Sciences, Brigham Young University, Provo, Utah 84097, The Chemical and Materials Sciences Division and the Environmental Molecular Sciences Laboratory, Pacific Northwest National Laboratory, P.O. Box 999, MSIN K8-96, Richland, Washington 99352, and the Brockhouse Institute for Materials Research, McMaster University, King Street West, Hamilton, ON L8S 4M1, Canada

Received: November 25, 2008

The recent controversy about the structure of liquid water pits a new model involving water molecules in relatively stable “rings-and-chains” structures against the standard model that posits water molecules in distorted tetrahedral coordination. Molecular dynamics (MD) simulations, both classical and ab initio, almost uniformly support the standard model, but because none of them can yet reproduce all of the anomalous properties of water, they leave room for doubt. We argue that it is possible to evaluate these simulations by testing them against their adherence to the bond-valence model, a well-known and quantitatively accurate empirical summary of the behavior of atoms in the bonded networks of inorganic solids. Here we use the results of ab initio MD simulations of ice, water, and several solvated aqueous species to show that the valence sum rule (the first axiom of the bond-valence model) is followed in both solid and liquid bond networks. We then test MD simulations of water, employing several popular potential models against this criterion and the experimental O–O RDF. It appears that most of those tested cannot satisfy both criteria well, except TIP4P, TIP4P/2005, and TIP5P. If the valence sum rule really can be applied to simulated liquid structures, then it follows that the bonding behaviors of atoms in liquids are in some ways identical to those in solids. We support this interpretation by showing that the simulations produce O–H···O geometries that are completely consistent with the range of geometries available in solids, and the distributions of instantaneous valence sums reaching the atoms in both the ice and liquid water simulations are essentially identical. Furthermore, we show that none of the extant asymmetric water potentials that produce “rings-and-chains” structures can satisfy our geometric criteria. Taken together, this is powerful evidence in favor of the standard distorted tetrahedral model of liquid water structure.

Introduction

The structure of liquid water has been difficult to describe with complete confidence because of a lack of experimental and theoretical constraints on proposed models. Until quite recently, experimental information about water structure has mainly been limited to X-ray and neutron scattering experiments, which provide radial distribution functions (RDFs) for atomic pairs and infrared spectroscopy, which can yield information about H-bond lengths. Neither of these yield unique descriptions of the H-bonded network.^{1–3} Theoretical constraints could be provided by quantum mechanics, but ab initio molecular dynamics (AIMD) simulations have been notoriously unsuccessful at reproducing the experimental RDFs^{4–12} and coefficients of diffusion.¹³ Even the use of hybrid exchange correlation functionals does not necessarily improve the ability of AIMD simulations to reproduce experimental data.¹⁴ Classical MD simulations have sometimes been more successful in this respect, but the empirical force fields utilized in these simulations have often been calibrated on experimental RDFs. Even where force-field calibrations have utilized quantum mechanical calculations, the fitted force-field parameters can in no way be regarded as unique solutions. Therefore, the bona fides of these simulations as true theoretical constraints are open to question.

The picture that has emerged from MD simulations of liquid water has been that each water molecule exists, on average, in distorted tetrahedral coordination, donating slightly more than two H bonds to neighboring molecules and accepting slightly more than two H bonds.^{1,2,11,15} (Coordination numbers like these are typically determined by integrating under the first peak in the O–O RDF or by some essentially arbitrary geometric definition of H bonds.) Although the results of MD simulations have always been open to question, this picture has been taken for granted because the results have been so consistent, even given force fields calibrated in different ways.

Recently, this picture of liquid water structure has been challenged as new types of experimental data have become available. Wernet et al.¹⁶ used X-ray absorption spectroscopy (XAS) and X-ray Raman spectroscopy at the oxygen K-edge for liquid water and ice to show that a prominent pre-edge feature in the spectrum for liquid water is nearly absent in the spectrum for bulk ice Ih but present in the spectrum for the ice Ih surface. Therefore, they reasoned that the H-bonded network in liquid water must be more like that of the ice surface (i.e., featuring many broken H bonds) than that of bulk ice Ih (i.e., with intact tetrahedral coordination of each water molecule). They used density functional theory (DFT) and the half-core-hole approximation for excited states to simulate the K-edge spectrum of an 11-molecule water cluster in various geometric configurations. They found that the pre-edge feature in question only appeared in configurations where a water molecule was donating a single H bond, defined by the following criterion

* Corresponding author. E-mail: barry_bickmore@byu.edu.

[†] Brigham Young University.

[‡] Pacific Northwest National Laboratory.

[§] McMaster University.

$$r_{\text{O-O}} \leq 3.30 - 0.00044\theta^2 \quad (1)$$

where $r_{\text{O-O}}$ is the O–O distance in angstroms and θ is $\angle\text{HO}\cdots\text{O}$ in degrees. Summing the spectra generated from the configurations examined, they found that approximately 80% ($\pm 20\%$) of the water molecules in liquid water had to be in single-donor configurations to fit the experimental spectrum at room temperature (298 K). By symmetry, approximately 80% ($\pm 20\%$) of the water molecules must accept only one undistorted/unbroken H bond. This, they argued, implies the presence of chain- or ring-like structures held together by a network of weaker H bonds.^{17–19}

Naturally, the claim that all theoretical models of water structure and dynamics put forth so far are wholly inaccurate has generated spirited discussion. Various groups have vigorously debated the suitability of the half-core-hole approximation for excited states to the water system,^{20–24} as well as the particular choice of cluster configurations used to model possible H-bond donor configurations.^{11,15,25,26} Others have interpreted X-ray scattering,²⁷ optical,²⁸ and photoelectron²⁹ spectra of water to support the standard model of water structure.

The intractability of this debate highlights an important problem. Most of the experimental techniques employed must be interpreted in light of molecular modeling techniques, but even ab initio techniques involve approximations that often render the interpretations questionable. The focus has therefore shifted back to the molecular modeling techniques themselves. Soper,³⁰ for example, reasoned that the only way to obtain long-lived chain structures in MD simulations of liquid water would be to employ water molecules with asymmetric distributions of electron density. He started with something similar to the standard SPC/E force field and incrementally shifted charge from the H on one side of the model water molecules to the H on the other. At each step, Soper refitted the force-field parameters to reproduce the experimental O–O RDF and tracked the number of H bonds (defined by eq 1) in the resulting simulations. He was able to produce an H-bond count of 2.2 per molecule (very close to the estimate of Wernet et al.¹⁶) when he placed a charge of $0e$ on one H atom and $-0.6e$ on the other, although this potential produces some strange features in the O–O RDF.³¹ Both supporters³² and critics^{31,33} of the rings-and-chains model have pointed out that such asymmetrical potentials produce radically unphysical results by various measures. Leetmaa et al.³² place the blame on the entire molecular modeling field, pointing out that no one has yet produced a theoretical simulation of water that quantitatively reproduces all of its physical properties.

Typically, empirical potentials for MD simulations of water are calibrated on one or more “target properties” of the substance. But because these potentials involve a number of adjustable parameters, the optimized values are not unique solutions, and the potentials may not work as well to predict other physical properties.³⁴ This obviously indicates that something is wrong with these potentials, but it is often difficult to say what. The point being made by those who promote a rings-and-chains model of water structure is that they believe that their spectroscopic results must lead us to question whether the H-bonded network structure of water is one of those physical properties extant water potentials do not predict all that well.

Rapaport³⁵ writes that “In the simulational context, understanding is achieved once a plausible model is able to reproduce and predict experimental observation.” If so, then the issue at hand is the extent to which standard water potentials produce structurally plausible results. To help address this issue, we introduce an additional geometric criterion for structural plau-

sibility: the valence sum rule. The valence sum rule is the first axiom of the bond-valence model, a venerable empirical theory in inorganic chemistry designed for the quantitative analysis of bond lengths in bonded networks.³⁶ The model was developed as a generalization of bonding geometries found in crystalline inorganic solids, for which average atomic positions can be determined very precisely via X-ray and neutron diffraction.

Should the same rules apply to bonding geometries in inorganic liquids? The bond-valence model has never before been rigorously applied to liquid bond networks. Therefore, after introducing the basic principles of the theory and showing how it can be used to constrain possible bonding configurations in solids, we demonstrate for the first time that the bond-valence model can be used to analyze configurations of H bonds in liquid water MD simulations quantitatively. We analyze a number of liquid water simulations to judge how well they conform to the valence sum rule and some related geometric criteria and derive some implications for the debate about liquid water structure. Whereas this type of analysis cannot definitively settle the debate, now we at least have a more complete basis for judging the structural plausibility of MD simulation results. And we can only claim to understand how water structure is linked to its properties to the extent that structurally plausible models reproduce experimental results.

Theoretical Background

The Concept of Valence. The bond-valence model³⁶ is, in essence, a quantitatively accurate version of Pauling’s second rule. Linus Pauling³⁷ formulated a set of rules to explain why some possible arrangements of atoms are found in inorganic crystals, whereas others have never been observed. He used simplified, abstract concepts like ionic “radius” and “valence” to simplify complicated quantum chemical interactions to a more intuitive level. The “valence” of an atom is a measure of its bonding power, or alternatively, a measure of the valence electron states available for bonding. Thus, atomic valence is equivalent to an atom’s oxidation state (e.g., the atomic valence of ferric iron is +3 and that of the chloride ion is -1). The average valence of the bonds formed by the cation (Pauling called it the “electrostatic bond strength”) can be calculated by dividing the cation valence by its coordination number. Pauling’s second rule (the valence sum rule) states that the sum of the electrostatic bond strengths around each anion in a crystal should be close to the anion valence. In other words, the atoms must be arranged so that all of their valence electron density (which defines their “bonding power”) is involved in bonding interactions with counterions. So, for instance, because Si^{4+} ions in the quartz ($\alpha\text{-SiO}_2$) structure are coordinated by four O^{2-} ions, the average valence of the Si–O bonds will be 1 valence unit (v.u.) Therefore, the O^{2-} ions must be bonded to exactly two Si^{4+} ions so that the two 1 v.u. bonds will counterbalance the -2 atomic valence of the O. (This also illustrates why bond valence concepts are typically applied to only inorganic systems; i.e., they cannot be applied to systems that include completely covalent bonding because the atomic valence of some atoms would be zero.) This simple rule works well to explain the coordination of atoms in a large number of inorganic crystal structures, but it turns out that one cannot use average bond valences in structures where there are severely distorted cation coordination polyhedra. It is intuitively obvious that shorter bonds should involve more of the valence electron density than longer bonds, and there is no reason to suppose that the correlation should be linear, so it is no surprise that average bond valences do not work well in such situations. To make

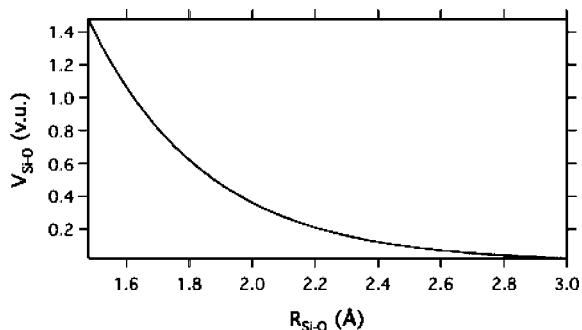


Figure 1. The valence of Si–O bonds in valence units (v.u.) plotted versus the length of the Si–O bonds, as calculated using eq 2 with $R_0 = 1.624 \text{ \AA}$ and $B = 0.37 \text{ \AA}$.³⁸

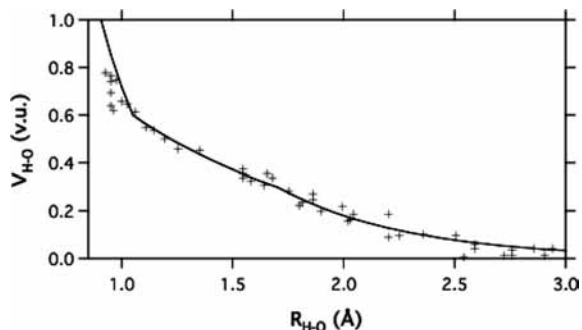


Figure 2. The valence of H–O bonds in valence units (v.u.) plotted versus the length of the H–O bonds. The line is calculated using eq 2 with $R_0 = 0.907 \text{ \AA}$ and $B = 0.28 \text{ \AA}$ for $R_{\text{H-O}} < 1.05 \text{ \AA}$, $R_0 = 0.569 \text{ \AA}$ and $B = 0.94 \text{ \AA}$ for $1.05 \leq R_{\text{H-O}} \leq 1.70 \text{ \AA}$, and $R_0 = 0.99 \text{ \AA}$ and $B = 0.59 \text{ \AA}$ for $R_{\text{H-O}} > 1.70 \text{ \AA}$, as recommended by Brown.³⁶ The data points are values obtained from valence analysis of bond lengths in crystal structures refined from neutron diffraction data.³⁶

the valence sum rule quantitatively accurate, subsequent work has focused on creating equations that accurately describe the relationship between bond length and valence.

Bond Length and Bond Valence. Brown and Altermatt,³⁸ for example, wrote a computer program designed to search the inorganic crystal structure databases and characterize the coordination polyhedra of a large number of cations. Given the valence sum rule, they were able to fit the following bond-length/bond-valence equation to this enormous data set

$$s = \exp\left(\frac{R_0 - R}{B}\right) \quad (2)$$

where s is bond valence in v.u., R is the bond length, and R_0 and B are fitted parameters specific to each cation–anion pair (e.g., a single pair of R_0 and B values is used for all Si–O bonds, but a different pair of values is used for Al–O bonds). Tables of the valence parameters for most common, and some uncommon, bond types have been published on the Internet (www.ccp14.ac.uk/ccp/web-mirrors/valence).

Bond valence versus length curves produced by eq 2 exhibit exponential decay; for example, the curve for Si–O bonds is plotted in Figure 1. The shape of the H–O bond valence versus length curve as determined via neutron diffraction studies is somewhat distorted because of the small size of the H^+ ion and resulting O–O repulsion effects.^{36,39} Therefore, Brown³⁶ recommends the use of three different sets of valence parameters for different regions of the curve. (See Figure 2.)

When these empirically derived equations, fitted to a large number of precisely known inorganic crystal structures, are used to calculate bond valences for particular crystal structures, the

calculated valence sums of bonds reaching ions in known crystal structures are typically within ± 0.1 v.u. of the atomic valences.³⁶ Larger deviations are indicators of a poor structure determination or internal stresses resulting from incommensurations among different parts of the structure. Given the sensitivity of bond valence to variations in bond length, this represents a stunning degree of accuracy. The bond-valence model is, therefore, routinely used to judge whether proposed molecular structures of inorganic solids (both crystalline and amorphous) are physically reasonable, whether the proposed structures were obtained via experiment or modeling.^{36,40–43} Although the valence sum rule cannot completely determine a structure, it does severely constrain acceptable combinations of bond lengths surrounding an atom.

Bond Valence in the Ionic Bonding Model. The physical basis of the bond-valence model has usually been explained in terms of the ionic model of bonding.^{36,44} Just as in classical MD simulations, the bond-valence model is a version of the ionic model in which atoms are treated as point charges that are prevented from coalescing by assuming the presence of an empirical two-body potential. But unlike the two-body potential model, which uses the electrostatic energy, the bond-valence model exploits the properties of the electrostatic field. The array of charges in both models is electroneutral, and the equilibrium geometry of the array is one in which cations are surrounded by anions and vice versa. The electrostatic field is represented by the electrostatic flux lines that link neighboring atoms, leading to a model based on nearest-neighbor interactions: cations are bonded to neighboring anions if they are linked by the electrostatic flux. The amount of flux linking any pair of ions (equated with the bond valence) obeys Gauss's law, which states that the total flux starting or terminating on a charge is equal to the charge. Therefore, in this context, Gauss's law is a restatement of the valence sum rule, and it holds true for any bonds that are not completely covalent in character.⁴⁴

This purely ionic description of bond valence was developed using simple electrostatics arguments involving arrays of point charges,⁴⁴ and yet it holds up quite well in the face of more sophisticated quantum mechanical treatments. Gibbs and co-workers have used quantum mechanical calculations of electron density distributions in Me–O bonded networks to show that there is an excellent linear correlation between bond valence and the electron density at bond-critical points.⁴⁵ This gives us confidence that bond valence accurately describes the amount of valence electron density involved in particular bonds (or equivalently, the electrostatic flux).

If both the bond valence model and the two-body potential model are based on the same physical picture of point charges held apart by repulsive potentials, however, then the question arises as to whether one can be used to check the calculations of the other. Will they not necessarily agree because both are based on the same assumptions? In fact, their differences are complementary. The two-body potential models have a single cost function, namely the total energy of the system. Because systems are chosen to include as large a number of atoms as it is feasible to calculate, the problem is highly underdetermined; several geometric configurations are likely to have energies close to the minimum so that the exact form of the potential becomes critical. The bond valence model, has a different cost function for each atom, and it is much less underdetermined. The exact form of the repulsive potential (in the form of the correlation between bond length and bond valence, eq 2) is therefore less important. If the two-body potential model represents a physicist's approach to the problem by summing the energy over all

atom pairs in the system, the bond valence model represents a chemist's picture of nearest-neighbor bonds exhibiting localized charge neutrality, as postulated originally by Pauling.³⁷ Of the many configurations that are consistent with the two-body potential model, only those that satisfy the valence sum rule are truly consistent with the model for structures in equilibrium.

Bond-Valence Model for Liquids. Because the bond-valence model quantitatively describes bond networks, there is no reason why the valence sum rule should not apply to any condensed phase of inorganic compounds, including liquids, which do not involve completely covalent bonds. But although the model has been quite successful for describing the molecular structures of inorganic solids, little has been done to apply it to liquid structures. There are good reasons for this, but the valence equations are capable of quantifying the strength of very weak interactions that go to the heart of debates about coordination numbers in condensed phases. It would be extraordinarily useful, therefore, to overcome the difficulties involved.

The main reason that the bond-valence model has only been applied in a very limited fashion to liquids is that bonding environments of atoms in liquids are much more flexible than those in solids. One of the major consequences of valence theory is the "distortion theorem," which shows that given the shape of the bond length versus valence curves (Figure 1) the average length of bonds reaching an ion must increase as its coordination polyhedron becomes more distorted.³⁶ Therefore, if the only information we can obtain about liquid structures involves average coordination environments, when the instantaneous structures can be strongly distorted, we cannot use the same valence parameters that we calibrated on the (less oscillatory) average atomic positions in solid crystals at room temperature.

The same problem arises when we treat crystal structures at high temperatures. Rising temperature causes stronger oscillations of the atoms in a crystal, allowing for greater instantaneous distortion. Therefore, average bond lengths necessarily increase to satisfy the valence sum rule. Because we can still experimentally obtain precise crystal structures at high temperatures, we can simply fit new valence parameters to the data at higher temperatures and create equations that relate the parameter values to temperature.³⁶

Our discussion of the consequences of the distortion theorem suggests one possible way to apply valence analysis to molecular simulations of liquids, where precise instantaneous interatomic distances can be obtained. If we assume that the oscillations of atoms in crystalline solids at room temperature are very small compared with those in liquids, then it might be possible to apply the valence parameters calibrated on average crystal structures to instantaneous structures in liquids. Here we report some fairly rigorous tests of this hypothesis.

Methods

The two main purposes of our study were to establish the fact that the bond-valence model can be quantitatively applied to MD simulations of liquid water and to use the valence sum rule to determine the structural plausibility of various water MD potentials that produce distorted tetrahedral coordination or rings-and-chains structures. To accomplish this, we had to perform several tasks: (1) We ran AIMD simulations of ice to (2) establish a valence-based cutoff criterion for defining H bonds in our simulations. (3) Next, we had to perform AIMD simulations of liquid water and a number of solvated oxo-molecules to demonstrate that the valence sum rule is obeyed in these simulated systems. (4) Finally, we ran classical MD simulations of liquid water using several common water

potentials and one asymmetric water potential to determine how well they conformed to the valence sum rule. Each task is described in more detail below.

Ab Initio Molecular Dynamics Simulations of Ice. We chose to use the gradient-corrected PBE96⁴⁶ exchange correlation functional for our AIMD simulations on the basis of the recommendation of Zhou and Truhlar,⁴⁷ who tested 44 DFT methods against a database of binding energies for nonbonded interactions. They found that the PBE96 functional performed even better than the hybrid DFT and MP2 methods tested. Similar results were obtained by Ireta et al.⁴⁸

The simulations were performed in the NVT ensemble using the Car–Parrinello method⁴⁹ using the pseudopotential plane-wave module in the NWChem program package.⁵⁰ The electron–ion interaction in these simulations, and those of aqueous systems described below, was approximated via the generalized norm-conserving pseudopotentials developed by Hamann⁵¹ (for atoms H, Be, B, C, O) or Troullier and Martins⁵² (for atoms Si, P, Cl, Fe), eliminating the need to calculate core electrons. These nonlocal pseudopotentials were modified to a separable form, as suggested by Kleinman and Bylander.⁵³ All of the simulations employed a fictitious electron mass of 1100 au, a cutoff energy of 110–114 Ry, and time steps of 5 au. All simulations were run for a total of about 1–5 ps. The ice simulation was run at a constant temperature of 270 K, maintained by means of Nosé–Hoover thermostats for the electrons and ions.^{54–58}

Because the hexagonal ice Ih structure is proton-disordered, we used the hypothetical "p-ice" structure,^{59,60} which is equivalent to the ice Ih structure except that it is proton-ordered with an orthorhombic unit cell. This hypothetical structure is specifically designed for quantum mechanical calculations.

Valence-Based H-bond Cutoff Criterion. Because eq 2 is an exponential decay function (Figure 1), in one sense, it does not really matter where we assign the cutoff distance for defining a bond as long as the distance is not too short. That is, lengthening the cutoff distance could drastically increase calculated coordination numbers but would not appreciably affect valence sums. One of the great strengths of the valence equations is that they are capable of quantifying very weak interactions, so we prefer to keep the cutoff distances as long as possible. With these points in mind, Brown³⁶ recommended a cutoff of 0.04 multiplied by the cation atomic valence, which neglects only very weak interactions and almost always produces the correct coordination numbers in cases where everyone agrees what they should be.

Bond cutoff distances obtained this way should not be taken too seriously, however. A number of years ago one of us (I.D.B.) examined the crystal structures of hydrates of perchloric acid⁶¹ and found that extremely weak H-bonding interactions of 0.01 to 0.02 v.u. (up to 3.1 Å H···O distance) could not be ignored if proper valence sums were to be maintained. Therefore, this serves to highlight the fact that the concept of coordination number is an artificial construct, and even if everyone agrees what a coordination number should be, there may be significant interactions with atoms outside of the coordination shell. In any case, with the bond-valence model, at least we have a universally applicable standard (the valence sum rule) by which we can decide when interatomic interactions are weak enough to ignore.

In this case, everyone agrees that the coordination number of O in ice ought to be 4.0, with two strong H–O and two weak H···O bonds reaching each anion. Therefore, we ran an AIMD simulation of ice to determine what the cutoff bond length should be for H···O bonds and chose the longest possible

TABLE 1: Average Valence of O–H ($V_{\text{O-H}}$) and H bonds ($V_{\text{H}\cdots\text{O}}$) Reaching Each O Atom in the p-ice *ab Initio* Molecular Dynamics Simulation, Average Total Valence of Bonds Reaching Each O atom (V_{Tot}) in the Simulation, and Average Coordination Number of the Water Molecules (N_{C})

$V_{\text{O-H}}$ (v.u.)	$V_{\text{H}\cdots\text{O}}$ (v.u.)	V_{Tot} (v.u.)	N_{C}
1.57	0.51	2.08	4.00

cutoff distance for defining H bonds that would yield a coordination number of 4.0 for O.

Ab Initio Molecular Dynamics Simulations of Aqueous Systems. We performed an AIMD simulation of 64 liquid water molecules under the same conditions as those of the p-ice simulation, except that the temperature was 300 K and the density was 1.00 g/cc. In addition, we performed AIMD simulations of H_4SiO_4 , H_3SiO_4^- , $\text{H}_2\text{SiO}_4^{2-}$, H_3PO_4 , H_2PO_4^- , HPO_4^{2-} , PO_4^{3-} , H_2CO_3 , HCO_3^- , and CO_3^{2-} with 30 to 31 water molecules and reported these results in a previous paper for a somewhat different purpose.⁶² Here the reason for reporting these simulations is that the valence available for $\text{H}\cdots\text{O}$ bonds on the O atoms of these molecules after accounting for the valence of O–H and Me–O bonds (here Me refers to cations other than H) varies widely. If we can show that the valence sum rule is closely followed in these AIMD simulations, as well as those of ice and liquid water, then our hypothesis will have passed a very exacting test.

Classical Molecular Dynamics Simulations. MD simulations were performed with a series of potential models, namely, the simple point-charge (SPC),⁶³ flexible SPC (SPC/Fw),⁶⁴ extended SPC (SPC/E),⁶⁵ transferable intermolecular potential (TIP) with three interaction sites (TIP3P),⁶⁶ flexible TIP3P (TIP3P/Fs),^{67,68} TIP with four interaction sites (TIP4P),⁶⁶ TIP4P/2005,⁶⁹ and TIP with five interaction sites (TIP5P)⁷⁰ models.

In each simulation, the cell contained 128 water molecules, and its volume was fixed to achieve a water density of 1.00 g/cc. All of the simulations were performed with the computer code DL_POLY⁷¹ in the microcanonical ensemble (NVE, i.e., constant number of particles, constant volume, and constant energy) at 298 K and zero applied pressure. The electrostatic interactions were calculated using the Ewald sum. A cutoff of 7.8 Å was used for the Lennard-Jones interactions. The trajectories were generated using the Verlet Leapfrog algorithm with a time step of 1 fs. All of the trajectories were propagated for 800 ps, and a configuration was collected every 0.2 ps for analysis. The first 100 ps were used to equilibrate the system and were therefore not included in the analysis.

Finally, we analyzed the trajectory file of an MD simulation (NPT) that employed Soper’s fully asymmetric potential (Soper-Asym). The software available to us could not accommodate this potential, so we analyzed output kindly provided by Professor Teresa Head-Gordon, run as described by Head-Gordon and Rick.³¹ In this simulation, the starting configuration consisted of 512 water molecules, where the O–H bonds were randomly assigned lengths with an average of 0.976 Å and a Gaussian distribution (SD = 0.07 Å) to match the experimentally determined O–H RDF. H–O–H bond angles were similarly randomly assigned about a mean value of 105.5°.^{31,72} The H1, H2, and O atoms in each molecule were assigned atomic charges of 0.6e, 0e, and –0.6e, respectively.^{31,72}

Results

O \cdots H Cutoff Distance. The AIMD simulation results for p-ice at 270 K are summarized in Table 1 and Figure 3. Figure 3a shows a histogram of the instantaneous valence of bonds

reaching the O atoms during the simulation divided into three categories: the strongest H bond reaching the O atom during a particular time step, the second-strongest, and the third-strongest. On the basis of these results, we chose a cutoff valence of 0.06 v.u. or 2.65 Å. This is as close as possible to Brown’s³⁶ general recommendation of 0.04 v.u. for monovalent cations, while producing an average coordination number of 4.00 for the water molecules. Given this cutoff distance, Table 1 reports the calculated average valence of O–H and $\text{H}\cdots\text{O}$ bonds reaching the O atoms, the average total valence of bonds reaching the O atoms, and the average coordination number of water molecules. (Averages were taken over all time steps and O atoms in the simulation.) The average total valence of bonds reaching the O atoms, 2.08 v.u., is within the expected range of 2.00 ± 0.10 v.u., and it would probably fall even closer to 2.00 v.u., if proton disorder were considered. Figure 3b shows a 3-D histogram of the frequency with which H bonds occurred with different combinations of $\angle\text{OH}\cdots\text{O}$ and bond valence.

Liquid Water Simulations. Table 2 summarizes the results of the MD simulations of liquid water, reporting the calculated average valence of O–H and H bonds reaching the O atoms, the average total valence of bonds reaching the O atoms, and the average coordination number of the water molecules as defined by our cutoff valence of 0.06 v.u. Figure 4 shows the O–O RDFs for all of the simulations compared with those from the neutron diffraction results of Soper⁷³ for water at 298 K. Significant variations are seen in the ability of the different simulations to reproduce the experimental RDFs and their adherence to the valence sum rule.

Instantaneous Valence Sums in the Water and Ice Simulations. Figure 5 shows histograms of the instantaneous total valence of bonds reaching the O atoms in the PBE96 p-ice simulation as well as the PBE96 and TIP5P liquid water simulations. In all three cases, the instantaneous valences are distributed normally about the average value, with standard deviations of 0.12 to 0.13 v.u.

Simulations of Aqueous Species. Figure 6 (adapted from ref. 62) shows a graph of the time-averaged $V_{\text{H}\cdots\text{O}}$ reaching the O atoms in the simulations versus average V_{u} . V_{u} is the “unsaturated valence” of the O atoms, meaning the valence of $\text{H}\cdots\text{O}$ bonds needed to satisfy the –2 v.u. valence of the O atoms after accounting for the valence of any O–H and Me–O bonds. The 1:1 line in the Figure indicates where the data points would fall if the valence sum rule was followed exactly. Clearly, the valence sum rule is followed closely, although a best-fit line through the data points would be shifted about 0.05 v.u. below the 1:1 line. This slight discrepancy, however, can be traced to Me–O bonds that are slightly too long, probably due to the incomplete description of van der Waals attractive forces in DFT methods.^{43,74}

Discussion

Valence Sum Rule in Liquids. Our AIMD simulations, taken together, provide compelling evidence of our hypothesis that the valence sum rule is followed in inorganic liquid bond networks. Furthermore, they show that we can use valence parameters derived from room-temperature average crystal structures to perform valence analyses of MD simulations of inorganic liquids as long as the valence sums calculated at each time step are averaged over the entire simulation. It is true that the dynamics of the systems are suspect: the AIMD simulation of liquid water performs rather poorly at reproducing the experimental O–O RDF. But given that the PBE96 functional does so well at predicting the energetics of H bonding^{47,48} and

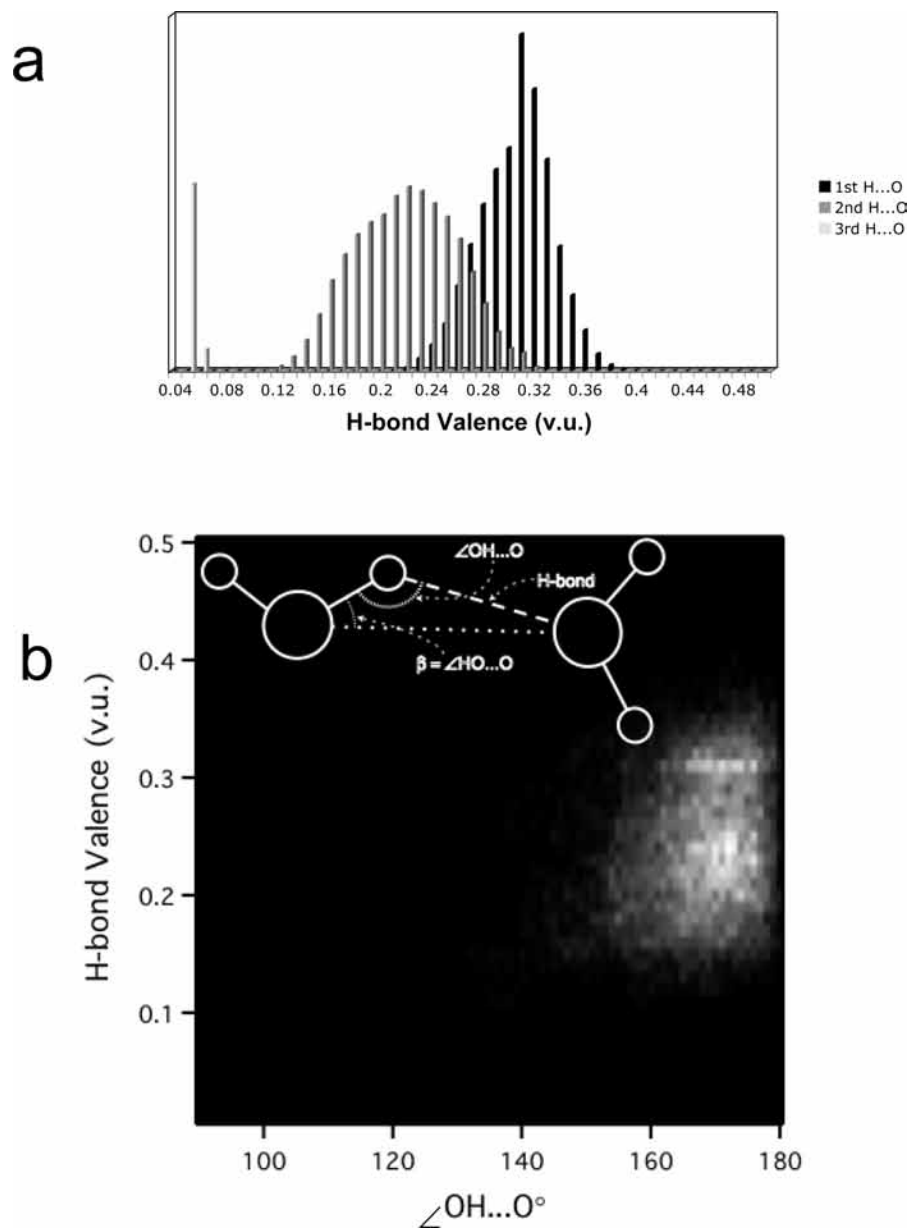


Figure 3. (a) Histogram of the valence of H bonds in the AIMD simulation of p-ice at 270 K. The first-, second-, and third-strongest H bonds reaching each O during a given time step are categorized separately. A cutoff distance of 0.06 v.u. for defining H bonds would yield a coordination number of 4.00 for water molecules in this structure. (b) 3-D histogram of the frequency with which combinations of H-bond valence and OH \cdots O angle ($\angle\text{OH}\cdots\text{O}$) appeared in the p-ice simulation. Brighter patches represent geometries with higher frequencies.

TABLE 2: Average Valence of O–H bonds ($V_{\text{O-H}}$), H bonds ($V_{\text{H}\cdots\text{O}}$), and Total Valence of Bonds Reaching Each O Atom (V_{Tot}) for the Liquid Water Molecular Dynamics Simulations as Well as the Water Coordination Numbers (N_{C}) as Defined by the 0.06 v.u. Cutoff Used Here

	$V_{\text{O-H}}$ (v.u.)	$V_{\text{H}\cdots\text{O}}$ (v.u.)	V_{Tot} (v.u.)	N_{C} (0.06 v.u.)
PBE96	1.65	0.36	2.01	4.23
SPC	1.43	0.41	1.85	4.39
SPC/Fw	1.30	0.47	1.77	4.36
SPC/E	1.43	0.43	1.87	4.37
TIP3P	1.67	0.37	2.04	4.43
TIP3P/Fs	1.56	0.42	1.98	4.46
TIP4P	1.67	0.40	2.07	4.35
TIP4P/2005	1.67	0.40	2.07	4.28
TIP5P	1.67	0.40	2.07	4.33
Soper-Asym	1.63	0.38	2.01	4.42

given that the O atoms in our AIMD simulations of p-ice, water, and aqueous oxo-molecules exhibited a very broad range of

valence available for accepting H \cdots O bonds (Figure 5) but still closely followed the valence sum rule, there is little room to question our main conclusions.

Evaluation of Common Water Potentials. To evaluate several common water potentials, we tracked both their adherence to the valence sum rule and their ability to reproduce the experimental O–O RDF. It is not an entirely straightforward process to extract RDFs for water from X-ray and neutron scattering data, and the peak shapes in published RDFs have varied considerably. However, the best available O–O RDFs, on the basis of synchrotron X-ray scattering¹ and neutron scattering⁷³ results, agree almost exactly. Therefore, these experimental O–O RDFs have commonly been used to assess the results of MD simulations. Soper⁷⁵ recently showed that the exact position and height of the first O–O RDF peak for water is very sensitive to instrumental error but that the subsequent peaks are quite well constrained by the best available data. Therefore, when evaluating the adherence of our simulated

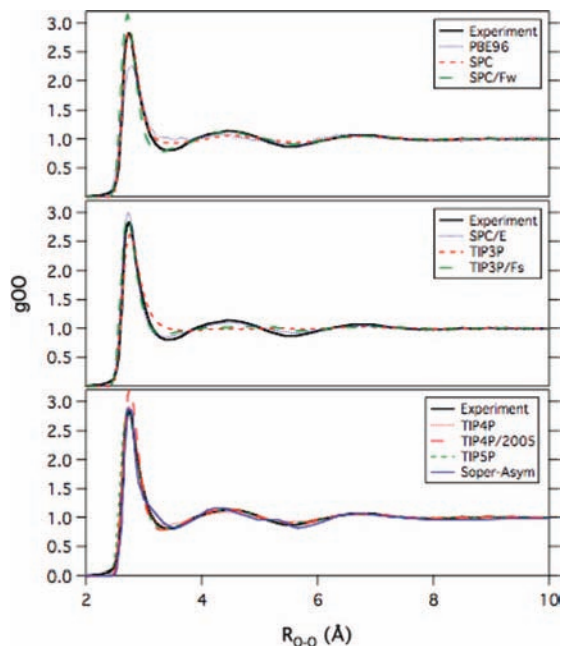


Figure 4. O–O radial distribution functions for the liquid water MD simulations reported here, compared with that obtained by analysis of neutron diffraction data by Soper.⁷³

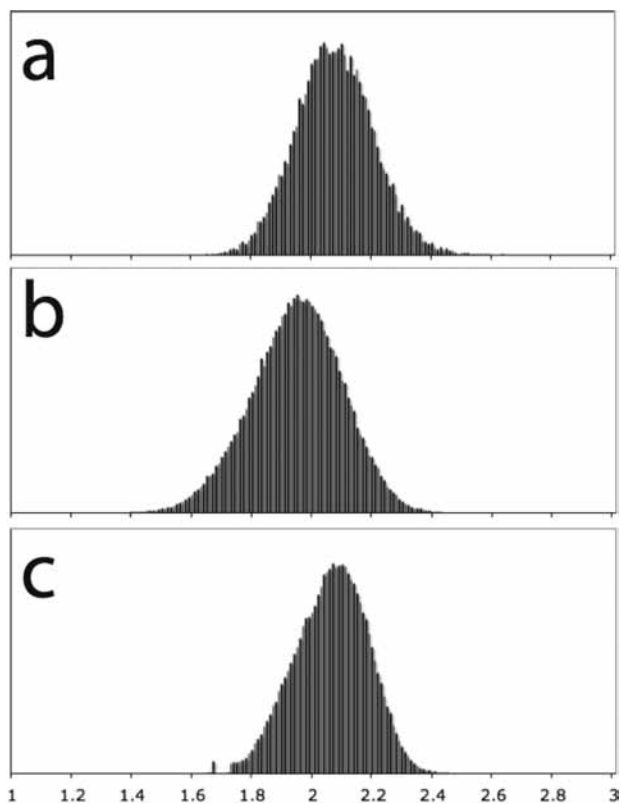


Figure 5. Histograms of the instantaneous total valence reaching O atoms in the (a) PBE96 p-ice simulation as well as the (b) PBE96 and (c) TIP5P liquid water simulations. The average values and standard deviations are, respectively, (a) $av = 2.07$ v.u., $SD = 0.13$ v.u., (b) $av = 2.01$ v.u., $SD = 0.15$ v.u., and (c) $av = 2.08$ v.u., $SD = 0.12$ v.u.

systems to the experimental O–O RDF, we paid more attention to the second and third peaks.

As shown in Table 2 and Figure 4, several of the classical MD simulations did quite well at mimicking the experimental O–O RDF (SPC/Fw, SPC/E, TIP4P, TIP4P/2005, and TIP5P),

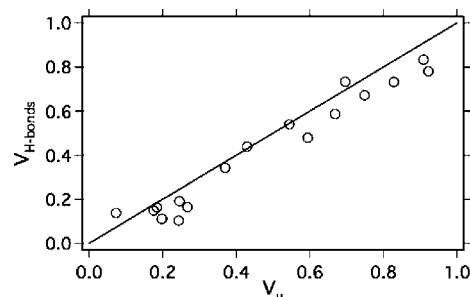


Figure 6. The time-averaged valence of H...O bonds reaching the O atoms of several solvated oxo-species in AIMD simulations plotted versus the “unsaturated valence” (i.e., the valence available for accepting H...O bonds) of these O atoms. The 1:1 line shows where the points would fall if the valence sum rule was exactly obeyed.

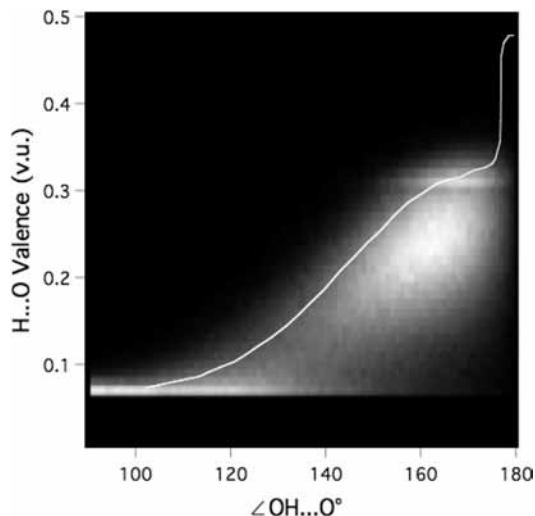


Figure 7. 3-D histogram of the frequency with which combinations of H...O valence ($V_{H...O}$) and OH...O angle ($\angle OH...O$) appeared in the TIP5P simulation, overlain by the solid white line. Brighter patches represent geometries with higher frequencies. The line represents the equilibrium H-bond geometries found in crystalline solids corresponding to the closest possible approach of the O atoms involved.

and several did well in adhering to the valence sum rule (TIP3P, TIP3P/Fs, TIP4P, TIP4P/2005, TIP5P, and Soper-Asym), yielding average valence sums of 2.00 ± 0.10 v.u. reaching the O atoms. However, only the TIP4P, TIP4P/2005, and TIP5P simulations can be said to have performed well by both measures. For example, the SPC/Fw and SPC/E simulations reproduced the experimental O–O RDF well but were significantly under-bonded with respect to the valence sums.

It is fair to say, then, that the TIP4P, TIP4P/2005, and TIP5P potentials produce structurally plausible results by these measures.

Incidentally, these two geometric criteria seem to present a fairly unified picture of water coordination. If we use the 0.06 v.u. cutoff criterion to determine the coordination number (N_c) of water molecules, we obtain values of 4.28 to 4.35 for the TIP4P, TIP4P/2005, and TIP5P simulations (Table 2). (The N_c values obtained for the other simulations are very similar.) The reason for this is illustrated in Figure 7, which shows a 3-D histogram of the frequency with which different combinations of $V_{H...O}$ and $\angle OH...O$ occurred in the TIP5P simulation. If we compare this plot with the p-ice histogram in Figure 3b, it can be seen that the bonds in the liquid water simulation are drawn out to more distorted geometries, and there is a high frequency of very weak bonds (~ 0.06 v.u.) due to bifurcation. RDFs give the probability of finding two atoms at a particular distance from one another relative to a completely random

distribution. Therefore, the integrated area $(4.7)^1$ of the first peak in the O–O RDF (Figure 4) is often equated with N_c because it seems likely that the greater probability of finding another O atom at certain distances from one another results from H bonding between the water molecules. These two types of N_c estimates yield very similar results; in fact, we would only have to lower the valence cutoff criterion for defining H···O bonds very slightly (i.e., to a value between 0.05 and 0.06 v.u.) to obtain exact agreement. Our conclusion is that the integrated area of the first O–O RDF peak really is a reasonably accurate estimate of the number of H-bonded neighbors surrounding a given water molecule.

Comparison with H-Bond Geometries in Solids. We can further support our claim that some standard water potentials are structurally plausible by comparing the H-bond geometries in the simulations with those found in crystalline solids. As we mentioned in the Introduction, our claim that the bond-valence model can be rigorously applied to liquids amounts to a claim that bonding geometries in liquids follow the same basic rules as those in solids. The main difference is simply that the molecules in liquids move around more. When we specifically examine the O–H···O bonding geometries in crystalline solids, we find that they present a special case. Brown⁷⁷ showed that because H atoms are so much smaller than O atoms, not every conceivable combination of H···O bond length and $\angle\text{OH}\cdots\text{O}$ is physically possible because the O atoms can only be packed so closely because of O–O repulsion. A very strong H bond (i.e., H···O valence is ~ 0.3 to 0.5 v.u.) cannot exist when the bond is strongly bent (i.e., $\angle\text{OH}\cdots\text{O}$ is closer to 90 than 180°) because the donor and acceptor O atoms would be forced too closely together (e.g., Figure 7). Naturally, this same criterion ought to apply to H-bonded liquids.

Brown^{36,77} quantified this criterion by cataloguing all of the O–H···O bonding geometries known at the time for crystalline solids and estimating a line representing the shortest H···O bond length observed for every $\angle\text{OH}\cdots\text{O}$. (The shortest possible H···O distance for a given bond angle would also necessarily correspond to the distance of closest O–O approach.) We have reproduced this line on top of the 3-D histogram of instantaneous O–H···O geometries observed in the TIP5P simulation (Figure 7). Here it is evident that the distance of closest approach in the simulation follows a very similar trend to that observed in crystalline solids but shifted slightly toward stronger, more bent bonds. This is only to be expected because the histogram represents instantaneous geometries, whereas the distance of closest approach line was derived from average atomic structures obtained by neutron diffraction. The atoms oscillate about equilibrium valence sums with a standard deviation of about 0.12 to 0.15 v.u. (See Figure 5.) Also, some very straight strong H-bond geometries observed in solids ($\angle\text{OH}\cdots\text{O} \approx 180^\circ$, H···O valence > 0.35 v.u.) do not occur in the liquid water simulation because these geometries only occur under rare circumstances.^{36,77}

The conclusion we draw from this comparison is that because the molecules in liquid water are relatively free to move about, they tend to sample essentially all possible O–H···O configurations. And the configurations available are essentially the same as those available in solid structures.

Instantaneous Valence Sums. The histograms of instantaneous bond valence (Figure 5) reaching the O atoms in the PBE96 p-ice, PBE96 liquid water, and TIP5P liquid water simulations, provide another striking confirmation of the idea that the bonding behaviors of atoms within liquids and solids are in some ways identical. Even though the molecules in liquid

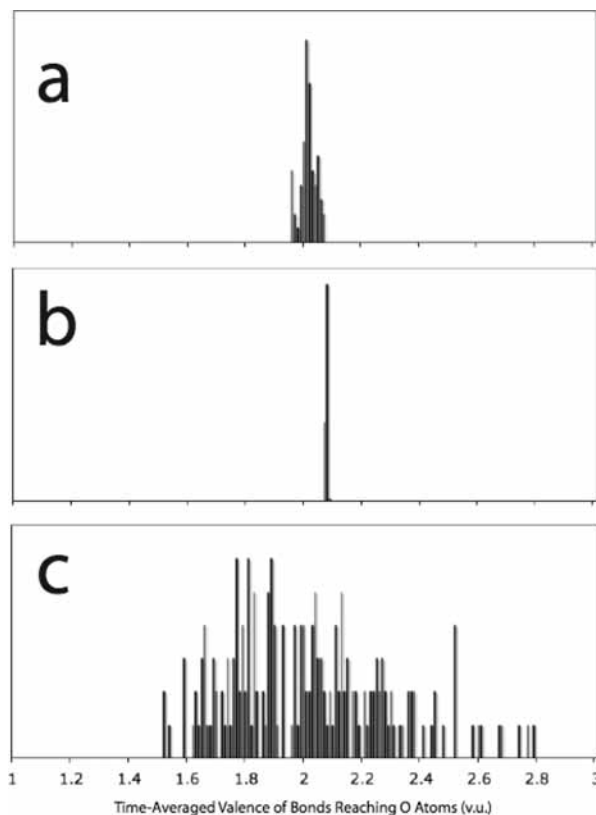


Figure 8. Histograms of the time-averaged valence of bonds reaching O atoms in the (a) PBE96, (b) TIP4P/2005, and (c) Soper-Asym MD simulations of liquid water. The valence sum rule is obeyed if the time-averaged valence sums are 2.0 ± 0.1 v.u. Whereas all of the O atoms in the PBE96 and TIP4P/2005 simulations pass this criterion, 75% of the O atoms in the Soper-Asym simulation fail.

water move about much more vigorously than those in ice (and the ice simulation was run at 30 K lower temperature), the bond networks in all cases seem to respond nearly identically, in terms of valence sums, to molecular motion. Only a certain amount of variation in the valence sums reaching the atoms is allowed,⁷⁸ and that amount does not appear to change much, even through a solid–liquid transition.

Evaluation of the Soper-Asym Potential. If some of the standard water potentials perform so well at achieving structural plausibility, then what of the asymmetric potentials that produce rings-and-chains structures? Soper's fully asymmetric potential (Soper-Asym) is, to our knowledge, the only asymmetric water potential that produces rings-and-chains structures in numbers similar to Wernet's original prediction and at least comes close to reproducing the experimental O–O RDF.^{16,30,31} (See Figure 4c.) But even though the O–O RDF was used as the target property to optimize this potential, it does not do well at predicting the second and third peaks, which are the most well constrained.^{31,75}

The apparent success of the Soper-Asym model at adhering to the valence sum rule (Table 2) is, in addition, deceptive. Although we reported that the average valence of bonds reaching all of the O atoms in the Soper-Asym simulation was 2.01 v.u., the valence sum rule applies to the coordination environments of individual atoms, and when we look at it from that perspective, we get a vastly different picture. Figure 8 shows histograms of the time-averaged valence of bonds reaching the individual O atoms in the PBE96, TIP4P/2005, and Soper-Asym simulations. The time-averaged valence of bonds reaching O atoms ranged from 1.95 to 2.07 v.u. in the PBE96 simulation

(Figure 8a), and from 2.06 to 2.08 in the TIP4P/2005 simulations (Figure 8b). That is, the time-averaged valence sums for all of the O atoms in these simulations were within the 2.0 ± 0.1 v.u. criterion. However, the time-averaged valence of bonds reaching the O atoms in the Soper-Asym simulation ranged from 1.51 to 2.78 v.u. (Figure 8c); 75% of the O atoms fail the valence sum criterion.

Because the Soper-Asym model fails both of our structural criteria, it is fair to say that it is not structurally plausible. However, our results offer some hope that it might be possible for someone to create asymmetric water potentials that improve on Soper-Asym in this respect.

In terms of the valence sum criterion, the main problem with the Soper-Asym potential seems to be the randomly assigned O–H bond lengths within the individual water molecules. Whereas the distribution of bond lengths might well be realistic on a time-averaged basis, the molecules are rigid, and the lengths of the O–H bonds reaching the H atoms have no correlation with the charge assigned to them. In reality, the shorter bonds would be more covalent, producing a lower atomic charge, but the distribution of lengths of O–H bonds reaching H atoms with atomic charges of $0.6e$ is statistically equivalent to that for those with atomic charges of $0e$. Therefore, the valence of $H\cdots O$ bonds donated by the H atoms has no correlation with the valence of O–H bonds reaching them, leading to a wider spread of valence sums. However, distribution of the time-averaged valence of $H\cdots O$ bonds reaching the O atoms in this simulation was relatively narrow: 97% of the $H\cdots O$ valence sums fell within 0.1 v.u. of the mean (0.38 v.u.).

If one wanted to create a structurally plausible asymmetric potential, then it would be necessary to assign longer O–H bond lengths to the H atoms with higher atomic charges. Then it might be possible to fit the other potential parameters to the O–O RDF, as Soper³⁰ did.

Simulation and Experiment. So far, we have focused exclusively on the issue of structural plausibility, but as we mentioned above, simulations do not produce understanding until a plausible model is able to reproduce and predict experimental observation.³⁵ Certainly, the two issues may be disconnected to some degree; for example, the structurally plausible models we have discussed (TIP4P, TIP4P/2005, and TIP5P) all involve rigid, nonpolarizable water molecules. However, it can be argued that only symmetric models are likely to do well at predicting experimental observations.

Given the growth in computing capability, it has become possible to target more and more properties when optimizing interatomic potentials. For instance, while optimizing the TIP4P/2005 potential, Abascal and Vega⁶⁹ targeted the temperature of the maximum density of water, the stability of water and various ice polymorphs with T and P , the enthalpy of vaporization of water, and the densities of water and various ice polymorphs at particular T and P values. Recently, Vega and Abascal³⁴ showed that TIP4P/2005 does very well at predicting vapor–liquid equilibria, the critical point, the shape and approximate position of the entire phase diagram for water and various ice polymorphs, T of maximum density of water and its variation in density up to 350 °C, the O–O RDFs for water and ice Ih, the densities of the ice polymorphs, the surface tension of water over a large T range, the equation of state of liquid water at high pressures, and the self-diffusion coefficient of water at 1 bar and 278–318 °C. It did not do as well at predicting the dielectric constant of water because the model is nonpolarizable.

The contrast between the success of TIP4P/2005 and the failures of Soper-Asym is patent. Head-Gordon and Rick³¹

showed that the Soper-Asym potential had to be run at 10 000 atm in an NPT simulation to produce an acceptable density of water. In other words, Soper-Asym water is a supercritical fluid under ambient conditions. Given these wildly inaccurate results, it seems that further attempts to adjust the model into structural plausibility would probably not bear much fruit in terms of predicting water's peculiar physical properties.

In fact, Chatterjee et al.⁷⁶ recently investigated the properties of SPC/E water in which the geometry of the molecules was systematically modified. They found that those versions of the model that produced distorted tetrahedral coordination for the water molecules could also produce some of the anomalous properties of water (e.g., the temperature of maximum density), whereas those versions that produced rings-and-chains structures could not. Therefore, it may be that the physical properties of water cannot be separated from a distorted tetrahedral framework.

So, whereas it may be possible to produce a structurally plausible asymmetric water model, it seems doubtful that such a model would be able to successfully predict much of the experimental data.

Conclusions

The recent debate about liquid water structure boils down to the question of whether we should trust standard water potentials to provide reasonably accurate descriptions of H-bond geometries. We argue that some of them (notably TIP4P, TIP4P/2005, and TIP5P) can be trusted for this purpose, even if they cannot quantitatively reproduce every physical property of water. We have supported this argument here by (1) using a suite of AIMD simulations to provide unequivocal evidence that the valence sum rule should be followed in liquids on a time-averaged basis and (2) showing that some standard water potentials (e.g., TIP4P, TIP4P/2005, and TIP5P) both fulfill this criterion and adequately reproduce the best O–O RDFs for liquid water. We have also shown that (3) none of the asymmetric water potentials proposed so far can pass either of these tests, and so we conclude that they are not structurally plausible. Next, we have argued that (4) while significant progress has been made in producing standard water potentials (e.g., TIP4P/2005) that are structurally plausible and reproduce many of water's peculiar physical properties, the distorted tetrahedral framework of the H-bonded network in water seems to be inextricably connected to those properties, so it appears unlikely that adjusting asymmetric potentials to achieve structural plausibility by our criteria will result in potentials that can accurately simulate water's properties.

We have also added weight to the structural plausibility of some standard water potentials by comparing the H-bond geometries they produce with those known to occur in crystalline solids. If the valence sum rule really can be applied to simulated inorganic liquid structures, then it follows that the bonding behaviors of atoms in these liquids are in some ways identical to those in the corresponding solids. We supported this interpretation by showing that (5) the simulations produce O–H \cdots O geometries that are completely consistent with the range of geometries available in solids, and (6) the distributions of instantaneous valence sums reaching the atoms in both the ice and liquid water simulations are essentially identical. So even though water molecules in the liquid move more vigorously, passing through a broader array of bonding geometries, the surrounding bond network responds in the same manner as in ice. (Note that we are not claiming that all inorganic liquid structures are necessarily as similar to their solid counterparts as water structure is to that of ice. Rather, we are claiming that

whatever bonding geometries are adopted in different condensed inorganic phases, they must follow some of the same rules, such as the valence sum rule.)

Taken together, we consider the above points to constitute a very strong argument in favor of the standard, distorted-tetrahedral model of water structure.

Finally, it is worth mentioning that the approach outlined here should be equally useful for judging proposed dynamic structures of other inorganic liquids and inorganic solid–liquid interfaces, which are notoriously difficult to characterize experimentally.

Acknowledgment. B.R.B. thanks the National Science Foundation (grant EAR-0525340) for supporting this work. A portion of this research was performed at EMSL, a national scientific user facility sponsored by the U.S. Department of Energy's (DOE) Office of Biologic and Environmental Research (OBER). K.M.R. acknowledges support from the DOE Office of Basic Energy Sciences (OBES) Geosciences Program and from the OBER for the Stanford Environmental Molecular Sciences Institute. Professor T. Head-Gordon kindly provided the output from a key MD simulation, and Professor A. Soper provided some helpful information about his work cited here. We also thank Johannes Lützenkirchen for providing the initial idea for this project and two anonymous reviewers for helping us improve the manuscript.

Supporting Information Available: Full version of ref 50. This material is available free of charge via the Internet at <http://pubs.acs.org>.

References and Notes

- Head-Gordon, T.; Hura, G. *Chem. Rev.* **2002**, *102*, 2651–2670.
- Ludwig, R. *Angew. Chem., Int. Ed.* **2001**, *40*, 1809.
- Stenger, J.; Madsen, D.; Hamm, P.; Nibbering, E. T. J.; Elsaesser, T. *Phys. Rev. Lett.* **2001**, *87*, 027401.
- Todorova, T.; Seitsonen, A. P.; Hutter, J.; Kuo, I. F. W.; Mundy, C. J. *J. Phys. Chem. B* **2006**, *110*, 3685–3691.
- Sit, P. H. L.; Marzari, N. *J. Chem. Phys.* **2005**, 122.
- VandeVondele, J.; Mohamed, F.; Krack, M.; Hutter, J.; Sprik, M.; Parrinello, M. *J. Chem. Phys.* **2005**, 122.
- Schwegler, E.; Grossman, J. C.; Gygi, F.; Galli, G. *J. Chem. Phys.* **2004**, *121*, 5400–5409.
- Kuo, I. F. W.; Mundy, C. J.; McGrath, M. J.; Siepman, J. I.; VandeVondele, J.; Sprik, M.; Hutter, J.; Chen, B.; Klein, M. L.; Mohamed, F.; Krack, M.; Parrinello, M. *J. Phys. Chem. B* **2004**, *108*, 12990–12998.
- Kuo, I. F. W.; Mundy, C. J. *Science* **2004**, *303*, 658–660.
- Grossman, J. C.; Schwegler, E.; Draeger, E. W.; Gygi, F.; Galli, G. *J. Chem. Phys.* **2004**, *120*, 300–311.
- Mantz, Y. A.; Chen, B.; Martyna, G. J. *Chem. Phys. Lett.* **2005**, *405*, 294–299.
- Fernandez-Serra, M. V.; Artacho, E. *J. Chem. Phys.* **2004**, *121*, 11136–11144.
- Fernández-Serra, M. V.; Ferlat, G.; Artacho, E. *Mol. Simul.* **2005**, *31*, 361–366.
- Guidon, M.; Schiffmann, F.; Hutter, J.; VandeVondele, J. *J. Chem. Phys.* **2008**, *128*, 214104.
- Smith, J. D.; Cappa, C. D.; Wilson, K. R.; Messer, B. M.; Cohen, R. C.; Saykally, R. J. *Science* **2004**, *306*, 851–853.
- Wernet, P.; Nordlund, D.; Bergmann, U.; Cavalleri, M.; Odelius, M.; Ogasawara, H.; Naslund, L. A.; Hirsch, T. K.; Ojamsae, L.; Glatzel, P.; Pettersson, L. G. M.; Nilsson, A. *Science* **2004**, *304*, 995–999.
- Bergmann, U.; Wernet, P.; Glatzel, P.; Cavalleri, M.; Pettersson, L. G. M.; Nilsson, A.; Cramer, S. P. *Phys. Rev. B* **2002**, *66*, 092107.
- Myneni, S.; Luo, Y.; Näslund, L.; Cavalleri, M.; Ojamäe, L.; Ogasawara, H.; Pelmenchikov, A.; Wernet, P.; Väterlein, P.; Heske, C.; Hussain, Z.; Pettersson, L. G. M.; Nilsson, A. *J. Phys.: Condens. Matter* **2002**, *14*, L213–L219.
- Näslund, L.; Lüning, J.; Ufuktepe, Y.; Ogasawara, H.; Wernet, P.; Bergmann, U.; Pettersson, L.; Nilsson, A. *J. Phys. Chem. B* **2005**, *109*, 13835–13839.
- Hetényi, B.; De Angelis, F.; Giannozzi, P.; Car, R. *J. Chem. Phys.* **2004**, *120*, 8632–8637.
- Cavalleri, M.; Odelius, M.; Nordlund, D.; Nilsson, A.; Pettersson, L. G. M. *Phys. Chem. Chem. Phys.* **2005**, *7*, 2854–2858.
- Wang, R. L. C.; Kreuzer, H. J.; Grunze, M. *Phys. Chem. Chem. Phys.* **2006**, *8*, 4744–4751.
- Prendergast, D.; Galli, G. *Phys. Rev. Lett.* **2006**, *96*, 215502.
- Iannuzzi, M. *J. Chem. Phys.* **2008**, *128*, 204506.
- Smith, J. D.; Cappa, C. D.; Messer, B. M.; Drisdell, W. S.; Cohen, R. C.; Saykally, R. J. *J. Phys. Chem. B* **2006**, *110*, 20038–20045.
- Odelius, M.; Cavalleri, M.; Nilsson, A.; Pettersson, L. G. M. *Phys. Rev. B* **2006**, *73*, 024205.
- Head-Gordon, T.; Johnson, M. E. *Proc. Natl. Acad. Sci. U.S.A.* **2006**, *103*, 7973–7977.
- Hermann, A.; Schmidt, W. G.; Schwerdtfeger, P. *Phys. Rev. Lett.* **2008**, *100*, 207403.
- Winter, B.; Aziz, E. F.; Hergenhanh, U.; Faubel, M.; Hertel, I. V. *J. Chem. Phys.* **2007**, *126*, 124504.
- Soper, A. K. *J. Phys.: Condens. Matter* **2005**, *17*, S3273–S3282.
- Head-Gordon, T.; Rick, S. W. *Phys. Chem. Chem. Phys.* **2007**, *9*, 83–91.
- Leetmaa, M.; Ljungberg, M.; Ogasawara, H.; Odelius, M.; Naslund, L. A.; Nilsson, A.; Pettersson, L. G. M. *J. Chem. Phys.* **2006**, *125*, 244510.
- Smith, J. D.; Cappa, C. D.; Wilson, K. R.; Cohen, R. C.; Geissler, P. L.; Saykally, R. J. *Proc. Natl. Acad. Sci. U.S.A.* **2005**, *102*, 14171–14174.
- Vega, C.; Abascal, J. L. F.; Conde, M. M.; Aragoes, J. L. *Faraday Discuss.* **2009**, advance article.
- Rapaport, D. C. *The Art of Molecular Dynamics Simulation*, 2nd ed.; Cambridge University Press: Cambridge, 2004.
- Brown, I. D. *The Chemical Bond in Inorganic Chemistry: The Bond Valence Model*; Oxford University Press: New York, 2002.
- Pauling, L. *J. Am. Chem. Soc.* **1929**, *51*, 1010–1026.
- Brown, I. D.; Altermatt, D. *Acta Crystallogr.* **1985**, *B41*, 244–247.
- Steiner, T.; Saenger, W. *Acta Crystallogr.* **1994**, *B50*, 348–357.
- Manceau, A.; Chateigner, D.; Gates, W. P. *Phys. Chem. Miner.* **1998**, *25*, 347–365.
- Shin, Y.-H.; Cooper, V. R.; Grinberg, I.; Rappe, A. M. *Phys. Rev. B* **2005**, *71*, 054104.
- Cooper, V. R.; Grinberg, I.; Rappe, A. M. In *Fundamental Physics of Ferroelectrics*; Davies, P. K., Singh, D. J., Eds.; American Institute of Physics: Melville, NY, 2003; pp 220–230.
- Bickmore, B. R.; Rosso, K. M.; Nagy, K. L.; Cygan, R. T.; Tadanier, C. J. *Clays Clay Miner.* **2003**, *51*, 359–371.
- Preiser, C.; Lösel, J.; Brown, I. D.; Kunz, M.; Skowron, A. *Acta Crystallogr.* **1999**, *B55*, 698–711.
- Gibbs, G. V.; Rosso, K. M.; Cox, D. F., Jr. *Phys. Chem. Miner.* **2003**, *30*, 317–320.
- Perdew, J. P.; Burke, K.; Ernzerhof, M. *Phys. Rev. Lett.* **1996**, *77*, 3865–3868.
- Zhao, Y.; Truhlar, D. G. *J. Chem. Theor. Comput.* **2005**, *1*, 415–432.
- Ireta, J.; Neugebauer, J.; Scheffler, M. *J. Phys. Chem. A* **2004**, *108*, 5692–5698.
- Car, R.; Parrinello, M. *Phys. Rev. Lett.* **1985**, *55*, 2471–2474.
- Apra, E.; et al. *NWChem: A Computational Chemistry Package for Parallel Computers*; Pacific Northwest National Laboratory: Richland, WA, 2005.
- Hamann, D. *Phys. Rev. B* **1989**, *40*, 2980–2987.
- Troullier, N.; Martins, J. *Phys. Rev. B* **1991**, *43*, 1993–2006.
- Kleinman, L.; Bylander, D. *Phys. Rev. Lett.* **1982**, *48*, 1425–1428.
- Bloch, P.; Parrinello, M. *Phys. Rev. B* **1992**, *45*, 9413–9416.
- Hoover, W. *Phys. Rev. A* **1985**, *31*, 1695–1697.
- Nosé, S. *J. Chem. Phys.* **1984**, *81*, 511–519.
- Nosé, S. *Mol. Phys.* **1984**, *52*, 255–268.
- Nosé, S. *Mol. Phys.* **1986**, *57*, 187–191.
- Casassa, S.; Ugliengo, P.; Pisani, C. *J. Chem. Phys.* **1997**, *106*, 8030–8040.
- Pisani, C.; Casassa, S.; Ugliengo, P. *Chem. Phys. Lett.* **1996**, *253*, 201–208.
- Brown, I. D. *Acta Crystallogr.* **1976**, *A32*, 786–792.
- Bickmore, B. R.; Rosso, K. M.; Tadanier, C. J.; Bylaska, E. J.; Doud, D. *Geochim. Cosmochim. Acta* **2006**, *70*, 4057–4071.
- Berendsen, H. J. C.; Postma, J. P. M.; van Gunsteren, W. F.; Hermans, J. In *Intermolecular Forces: Proceedings of the Fourteenth Jerusalem Symposium on Quantum Chemistry and Biochemistry Held in Jerusalem, Israel, April 13–16, 1981*; Pullman, B., Ed.; Reidel: Dordrecht, The Netherlands, 1981; pp 331–342.
- Wu, Y.; Tepper, H. L.; Voth, G. A. *J. Chem. Phys.* **2006**, *124*, 024503.
- Berendsen, H. J. C.; Grigera, J. R.; Straatsma, T. P. *J. Phys. Chem.* **1987**, *91*, 6269–6271.
- Jorgensen, W. L.; Chandrasekhar, J.; Madura, J. D.; Impey, R. W.; Klein, M. L. *J. Chem. Phys.* **1983**, *79*, 926–935.
- Schmitt, U. W.; Voth, G. A. *J. Chem. Phys.* **2000**, *111*, 9361–9381.

- (68) Dang, L. X.; Pettitt, B. M. *J. Phys. Chem.* **1987**, *91*, 3349–3354.
(69) Abascal, J. L. F.; Vega, C. *J. Chem. Phys.* **2005**, *123*, 234505.
(70) Mahoney, M. W.; Jorgensen, W. L. *J. Chem. Phys.* **2000**, *112*, 8910–8922.
(71) Smith, W. R.; Todorov, I. T. *Mol. Simul.* **2006**, *32*, 935–943.
(72) Soper, A. K. *Chem. Phys.* **1996**, *202*, 295–306.
(73) Soper, A. K. *Chem. Phys.* **2000**, 258, 121–137.
(74) Wu, X.; Vargas, M. C.; Nayak, S.; Lotrich, V.; Scoles, G. *J. Chem. Phys.* **2001**, *115*, 8748–8757.
(75) Soper, A. K. *J. Phys.: Condens. Matter* **2007**, *19*, 335206.
(76) Chatterjee, S.; Debenedetti, P. G.; Stillinger, F. H.; Lynden-Bell, R. M. *J. Chem. Phys.* **2008**, *128*, 124511.
(77) Brown, I. D. *Acta Crystallogr.* **1976**, *A32*, 24–31.
(78) Aquino, A. J. A.; Tunega, D.; Haberhauer, G.; Gerzabek, M. H.; Lischka, H. *Geochim. Cosmochim. Acta* **2008**, *72*, 3587–3602.

JP810364T